Twelfth USA/Europe Air Traffic Management Research and Development Seminar (ATM2017)

A simple method to integrate Mode S Indicated Airspeed with Ground Based Trajectory Prediction

Bram Vandermeersch, Jonathan Marmont
Commercial Services & Delivery, R&D
NATS
Whiteley, UK
Bram.Vandermeersch@nats.co.uk

Abstract— **Decision support tools in the London Area Control Centre rely on trajectory prediction to provide the Air Traffic Control Officers (ATCO) with a manner to quickly identify potential interactions between aircraft. These tools are underpinned by a trajectory predictor.**

Research has shown that more accurate inputs to these TP algorithms yield more accurate results. Previous research has focussed on aircraft mass and more accurate meteorological data. This study investigated the effect of including downlinked Mode S Indicated Airspeed (IAS) as a Calibrated Airspeed (CAS) value into the TP calculation. The effect was measured on the accuracy and stability of the prediction during the climb portion of each flight. Five potential approaches were implemented in a MATLAB test harness and the performance was compared against the accuracy and stability of the Eurocontrol Base of Aircraft Data (BADA) baseline implementation.

Analysis of 2,219 climb segments from 715 flights which departed from UK airports resulted in almost 280,000 performance points, distributed over the six TP models. These results show that the effect of including Mode S IAS on the vertical accuracy is marginal. The along track accuracy shows significant improvement when Mode S IAS is included. The inclusion of Mode S IAS does have a detrimental effect on the TP CAS stability as the CAS is no longer a constant.

Of the five approaches, a one dimensional Kalman filter shows most promise in terms of trade-off between TP accuracy and CAS stability. Furthermore the Kalman filter should be easier to prove in a safety environment and expanded to include other parameters in order to provide better accuracy and performance.

Keywords Aircraft Trajectory Prediction, Conflict Detection and Resolution, Mode-S, Speed Intent

I. INTRODUCTION

Controllers at NATS London Area Control Centre are supported by a suite of electronic tools to assist in the management of UK en route air traffic and the provision of separation between aircraft. The three principle components underpinning these electronic decision support tools are Trajectory Prediction (TP), Medium Term Conflict Detection (MTCD) –sometimes referred to as conflict detection and resolution (CDR) - and Flight Path Monitoring (FPM). The TP uses a simple point-mass model [1] that is integrated in time to create four dimensional prediction paths of up to 18 minutes in length. This trajectory is of sufficient length to assist the ATCO in separating and monitoring aircraft for their particular area and traffic flows of responsibility. The MTCD compares a set of trajectories for each aircraft against all others deemed to be of interest for that airspace sector. A set of pairwise potentially interacting aircraft are then identified which is then distilled down using rules from standard operating methods for ATC and others, to yield a set of valid interactions that enable the ATCO to both monitor aircraft and makes good decisions if tactical intervention is required. This final filtered interaction list is then displayed to the ATCO using plotting techniques that are specific to the task begin performed by the ATCO at that time. The FPM function monitors for aircraft deviations from route and deviations from current ATC clearance (if issued). The FPM creates its own prediction class of TP allowing it to be compared alongside all other trajectory classes in MTCD, this approach allows the tools to consistently provide a full level of monitoring and decision support even in situations of multiple deviations e.g. in cases of strong winds aloft.

Relevant information from the TP, MTCD and FPM is presented to the ATCO in a number of tools; the most significant being the separation monitoring display (SM) and the level assessment display (LAD). The SM maintains an accurate picture of when and where pairs of relevant aircraft will be closest to one another, with plotting rules distinguishing between predicted losses of separation, potential losses of separation (using a predicted trajectory uncertainty) and no loss of separation. The LAD populates when aircraft are selected by the ATCO and is an aid to enable the ATCO to make good judgements when instructing level changes to aircraft, this has been seen to enable earlier and more efficient climb clearances and more optimal descent profiles while ensuring the safe operation of the sector.

The greater the accuracy of an initial aircraft state, the less uncertainty will be propagated with the nominal prediction(s); less uncertainty will ultimately present fewer potential interactions for the ATCO to monitor and understand in a given scenario for the toolset described above. It is a generally accepted hypothesis that ATCOs, by using such a system, will be able to control more aircraft (i.e. increase the capacity of the airspace) and/or provide more efficient profiles to airlines (reducing fuel burn and CO2 emissions). Such benefits are not constrained to a tactical timeframe, with strategic functions, such as network, flow and queue management able to take advantage of reduced prediction uncertainty also.

The initial aircraft state and aircraft intent are approximated using the aircraft performance model, radar information, ATC instructions (if issued) and route information. Atmospheric conditions (temperature and wind forecasts) are also estimated, as derived from a forecast MET model. The ground based prediction system does not use any specific aircraft data for a given flight, including any updates from the aircraft when in flight that can be used to improve the TP accuracy (although FPM will benefit from SFL data sent via Mode-S). Approximations for aircraft mass and speed then must be made (amongst others), but these are neither operator nor route specific, which leads to significant prediction uncertainty in order to maintain the required level of prediction containment useful to the ATCO. Flight deck throttle setting, bank angle, rate of climb/descent etc, as required by the performance model, are all approximated in a similar way. As such the reference data that is currently available to ground systems for TP has the potential to be greatly improved; any such improvements will in turn facilitate greater accuracy in the nominal predictions and associated reductions in prediction uncertainty.

When the aircraft and ground systems are equipped to facilitate downlinked data the ability to share the on-board trajectory data according to the contract terms of the Air Navigation Service Provider (ANSP), will be possible. One example of this is the ADS-C EPP ‘extended projected profile’ concept which has seen some promise in studies [2], [3] and in flight trails [4] and is an important part of the SESAR Concept of Operations serving the European ATM Masterplan[5], however the deployment target for EPP as part of the ATN B2 services is 2024, leaving some years before European airspace can benefit from such equipped flights.

The Aircraft Intent Description Language [6] formalised the aircraft intent for transmission to the ground systems. This meta-language for aircraft intent description is a vastly scalable approach which suits the needs of current ATC and the needs of a future, more automated ATC system. However transmission of this data also relies on established air-ground data sharing links, such as ATN B2, which are not yet available.

Improving the accuracy of the mass, speed and met data for aircraft will produce the greatest benefits in the near term. Machine Learning has been applied to improve the accuracy of mass [7] and speed predictions [8] to good effect and has done so using only data that is currently available to the ground system. Aircraft compliant with Aircraft equipped with Mode-S Enhanced Surveillance (EHS) are now prevalent in UK airspace and provide the basic functionality features and eight downlinked aircraft parameters; this data includes aircraft indicated airspeed (IAS), ground speed (GS) and Vertical Rate (VR). Using Mode-S derived winds aloft data from the aircraft, met predictions are expected to benefit greatly here [9], [10], which will improve ground based TP.

This study presents a simple treatment for using Mode S downlinked IAS to improve the ground based trajectory prediction used by a decision support tool set for the ATCO, this is assessed using accuracy and stability metrics defined herein. This paper compares the performance of a standard TP implementation with the performance of five other approaches that utilise Mode-S IAS for the climb phase only. The paper will first discuss the method used to undertake the analysis, followed by a description of the evaluated approaches. The results are in section III followed by conclusions and recommendations for further work

II. METHODOLOGY

The merits of five approaches to incorporate downlinked Mode-S IAS into the trajectory prediction calculation were investigated. To evaluate the merits of each approach the effects on prediction accuracy and stability were measured on a representative sample of data. As outlined in Figure 1, the investigation was undertaken in a specifically developed a software pipeline. The software pipeline (written in the MATLAB environment) extracted the relevant flight information, selected valid flight segments and computed the TPs:

A. *Filtering Criteria*

In order to evaluate a representative sample that would test the performance of downlinked aircraft parameters, data was extract from a “typical” busy period of UK air traffic activity. The analysis was limited to include only flights during climbing phase as the procedures during descent are significantly more complex. In total a total of 715 flights taking off from eight UK airports were included in this study. Nearly 75% of the flights departed from London Heathrow or London Gatwick and just over 50% were A319 or A320 type aircraft. The distribution of aircraft types is shown in Figure 2 This distribution is typical for flights departing in the London FIR.

B. *Valid Segment Detection*

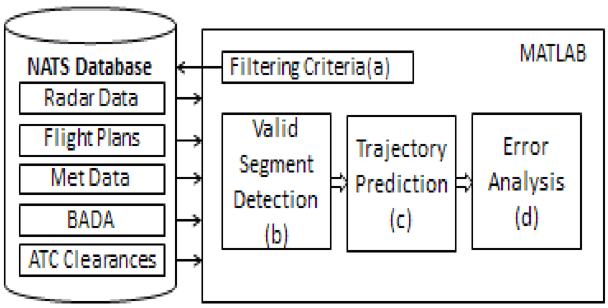

Figure 1 Overview of the data extraction pipeline.

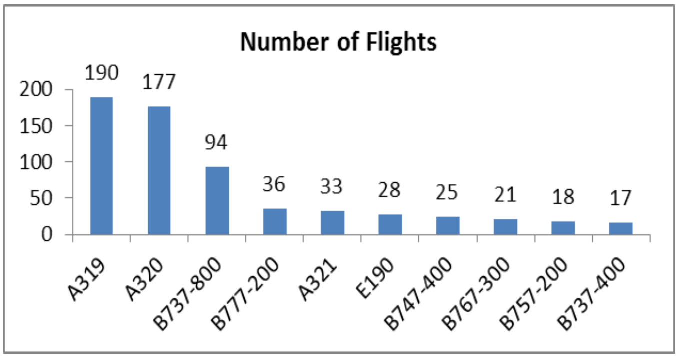

Figure 2 Ten most prevalent aircraft types in the dataset

Figure 3 shows the way a valid segment was selected. During a flight aircraft typically receive multiple clearances. Each new clearance invalidates at least a portion of the previous clearance. The portion of the prediction that occurs after a subsequent clearance was issued can no longer be evaluated as its relevancy was superseded. The portion of flight between two ATC instructions is known as a "valid segment".

The majority of aircraft types are in UK airspace are limited to 250KIAS when below 10,000ft. Furthermore when the conversion altitude is reached the aircraft no longer maintain a constant CAS. Therefore the study focussed on clearances which were issued above 10,000ft and before conversion altitude was reached. In this study the conversion altitude is the altitude where the CAS starts decreasing consistently.

A restriction was placed on the length of the valid segment to ensure there was enough meaningful data to analyse. A segment was only considered for analysis if it lasted for at least 30 seconds. This process resulted in 2,219 valid segments over the 715 flights.

C. Trajectory Prediction

To predict trajectories with various speed models a baseline TP was developed within the MATLAB numerical environment. This allowed for an environment in which a new concept could easily be implemented and evaluated. The TP implementation was based on the EUROCONTROL Base of Aircraft Data (BADA) version 3 [1]. BADA is a point mass total energy model. The model uses lookup values for speed, mass and other performance parameters. The nature of the TP means the prediction does not adapt if the aeroplane deviates from its nominal performance behaviour [11].

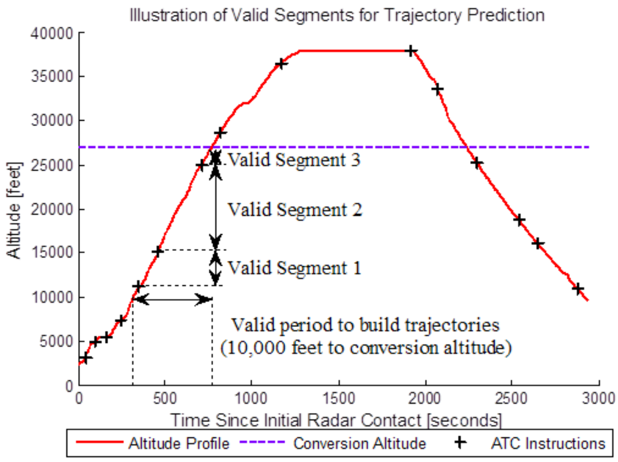

Figure 3 Valid segments during the climb portion of a flight

The standard BADA approach decides on a value for climb CAS from a lookup table, based on a set of input parameters. This study investigated the effect of integrating the Mode S IAS into the TP calculations for the climb portion; therefore the implementation had to be modified. The implementation used for this study allowed different ways to calculate a value for climb CAS. The different approaches to calculate a climb CAS are described in Subsection II.D.

To assess the influence of the introduction of Mode S IAS on the predicted climb profile the data for each approach was generated. This step is shown in Figure 1 (c). Each of the 2,219 segments has lateral, vertical and speed clearance information as well as the radar data covering the segment. A trajectory was generated for each radar return. Each radar return was taken as the initial condition of a TP. The results from this step were used in Section III for the error calculation.

D. Proposed Methodologies for CAS Calculation

During the TP, the calculation is initialised with a CAS value which is kept constant throughout the climb portion of the prediction. This leads to the true airspeed (TAS) increasing with the aircraft altitude. The predictions in this study end when the transition altitude is reached, as per II.B.

In theory, once the 250kts speed restriction at 10,000ft is lifted the aeroplane's crew or FMS chooses an airspeed value and a power setting based on mass, economy settings and potentially other operator preferences. The autopilot then maintains this airspeed by pitching up or down.

In reality, the profile of an aeroplane in a climb typically looked like Figure 4. This plot shows the received Mode S IAS during a climb for a Boeing 777-200 from London Heathrow to Kotoka, Ghana. The Mode-S IAS remained constant at the 250KIAS mark until the aeroplane reached 10,000ft at which point the aeroplane accelerated to 270KIAS at t=350s. A further 100 seconds later (t=450s) the aeroplane accelerated further to 295KIAS. The CAS component of the TP has to accommodate these changes in Mode-S IAS during the climb. In addition to the big step changes, which are less common, the Mode S IAS graph shows higher frequency noise in the segments where the Mode S IAS would be considered constant.

For the analysis six approaches were implemented in the MATLAB test harness. Each of these approaches is described below:

1. **BADA:** This is the baseline speed model. A value is selected based on the circumstances from a lookup table. The CAS value is assumed to remain constant throughout the climb until the conversion altitude is reached. Any other CAS approaches were compared against the results generated by this approach.
2. **S-CAS** (Stable CAS): is an engineering approach which chooses either the Mode S IAS as CAS or the BADA

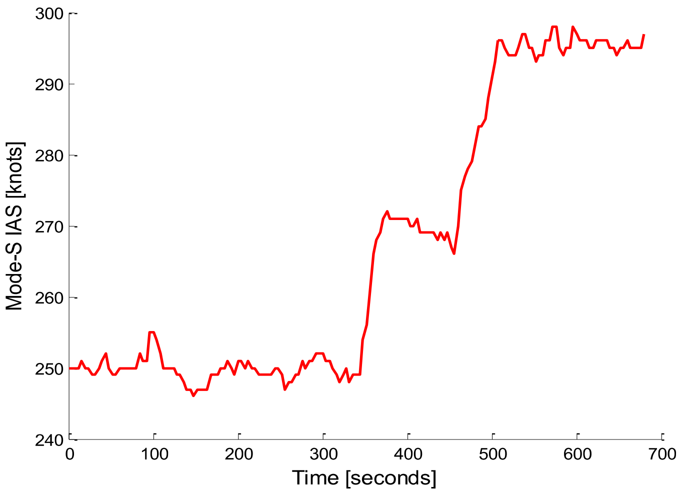

Figure 5 A typical Mode S IAS profile

CAS. The chosen value remains constant throughout the climb. The algorithm first determines whether the downlinked Mode S IAS is stable. This is the case if the value has been within a certain threshold for a number of samples. If these conditions are met the stable Mode S IAS value is selected as the climb CAS. If the Mode S IAS fluctuated too much the algorithm reverts back to using BADA CAS as the selected value for the climb CAS.

3. **IAS** In this approach the latest downlinked Mode-S IAS is directly used as the climb CAS. No signal conditioning is performed. Unfiltered CAS (IAS): In this approach the algorithm uses the last received Mode S IAS value as the initial CAS value for the prediction.
4. **LPF**: The Low Pass Filter method uses a combination of a finite and an infinite impulse response (FIR, IIR) filter. The FIR filter has been designed to eliminate the higher frequency noise of the Mode-S IAS value. When step changes are detected a tuned IIR filter deals with the low frequency changes. The filters were designed by doing a frequency spectrum analysis on the raw CAS values. Filter parameter values were chosen using the MATLAB Filter Builder which is part of the DSP System Toolbox.
5. **Kalman** Filter: A value for the initial CAS is generated by calculating a weighted average between the previous state estimation and the downlinked value. The relative importance of the new measurement depends on the covariance of previous measurements and is updated on each iteration. This study evaluated the use of a one dimensional Kalman filter. The Kalman filter only included estimated a value for CAS based on downlinked Mode S IAS.
6. **GMA**: The final approach is the Growing Mean Average (GMA). This algorithm is similar to the S-CAS algorithm. The method uses the stable Mode S IAS value if the received value has been within a certain threshold from the other readings. If the threshold is crossed the method reverts to using the raw value of the downlinked value.

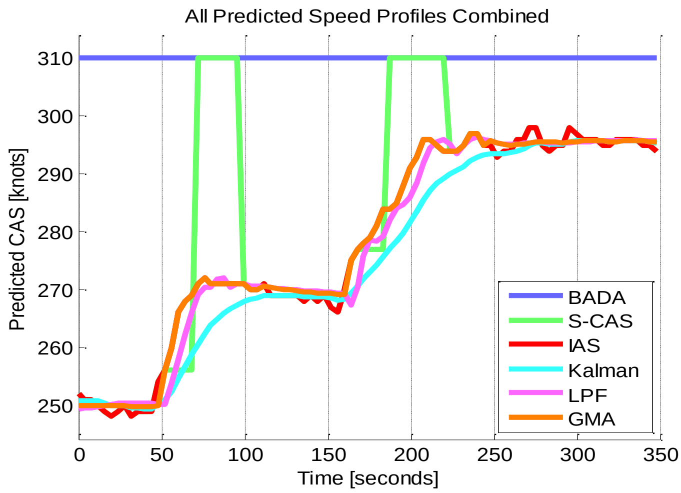

Figure 4 The resulting CAS profiles from the Mode S IAS information

Figure 5 shows the same example speed profile from Figure 4. The baseline BADA model predicts 310kts CAS throughout the whole valid segment. The S-CAS line shows the discontinuities in CAS values when the aeroplane accelerates and the model has to temporarily revert back to BADA CAS.

The LPF and GMA approaches show a value which follows the raw Mode-S IAS quite closely but eliminates some of the higher frequency responses. The Kalman filter's response can be seen to be slower; however, the filter's parameters were specified deliberately to achieve this in order to investigate the effect of an increased delay but improved CAS stability by focussing on eliminating the higher frequency noise.

III. Results

A measurement of the trajectories using all the six models to calculate a more appropriate CAS estimate resulted in roughly 280,000 data points. The performance of the TP on ATC operations was evaluated using a set of metrics. The metrics measure accuracy and stability. In this section the results are shown per metric.

The main way to demonstrate the result is by using boxplots. The chosen format for these boxplots was to use the whiskers at the 5th and 95th percentile. The box itself shows the quartile and the '+' sign indicates the mean of the dataset.

A. Normalised vertical error

To assess the vertical error of the prediction, a normalised vertical error metric was designed. The metric was designed to compensate for the difference in length of the segments.

$$\hat{\varepsilon}_{vertical} = \frac{|Trapezoidal\ Area\ Between\ Curves|}{(VRDD \times VRPL)} \qquad (1)$$

$$\bar{\varepsilon}_{error\ type} = \frac{n_1\mu_1 + n_2\mu_2 + n_3\mu_3 + \cdots + n_p\mu_p}{n_1 + n_2 + n_3 + \cdots n_p} = \frac{\sum_{p=1}^{Q} n_p\mu_p}{\sum_{p=1}^{Q} n_p} \qquad (2)$$

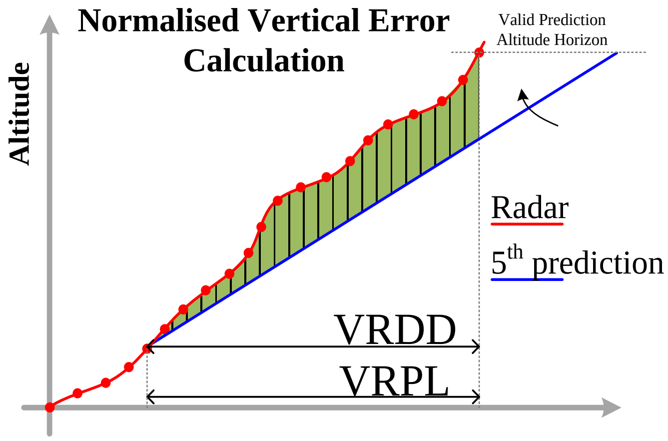

Figure 7 Normalised vertical error calculation

The calculation of the vertical error metric is shown in Figure 7 and reflected in (1). The difference between the prediction and the actual altitude profile from radar is integrated over time. This resulting value is scaled for its length by dividing it by the Valid Remaining Down track Distance (VRDD) and the Valid Remaining Prediction Lifetime (VRPL). This makes the measure dimensionless and allows for longer and shorter segments to be compared. The errors are combined through a weighted average using (2).

Figure 6 shows that there is no significant difference between the BADA baseline and the methods which incorporate Mode S IAS. The errors in the BADA baseline equate to approximately 500 feet/min, whereas for models using Mode-S data, the means range from 464 – 468 feet/min. Each of the new methods results in a 13-15% reduction of the median error value and an 11% reduction of the mean error.

B. Along track error

The along track error is measured in the time domain. The prediction is compared against the flown radar track. The radar samples are compared to the prediction by calculating at which predicted time the prediction is abeam the location of the sampled radar point at that time according to (3). The

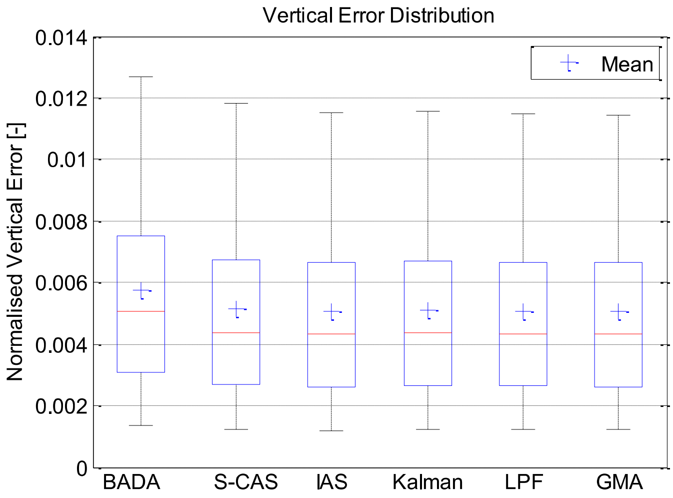

Figure 6 Vertical Error for each of the approaches

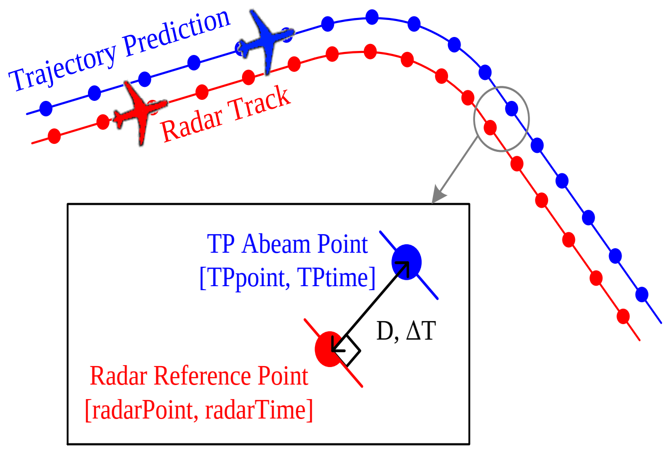

Figure 8 Along Track Error Calculation

geometry is shown in Figure 8. The errors are measured in sec/min.

$$\varepsilon_{\text{along track}} = \frac{|\text{Radar time} - \text{TP time}|}{(\text{TP look ahead time })} \qquad (3)$$

The time errors are normalised by dividing the error by the TP look-ahead time. This means that the error becomes a fraction of the length along the trajectory. The relative error is averaged over all the evaluation points along the trajectory for each prediction using (2).

The along track error distribution is shown in Figure 9. The result shows that including the Mode-S IAS in the TP algorithms shows a significant reduction in error. The standard BADA TP has a mean error of 4.6 sec/min whereas including the Mode S speed reduces this to a values ranging from 2.2 sec/min to 1.9 sec/min. Also the spread in results is much reduced for the algorithms which include Mode S IAS.

C. CAS stability

Figure 9 shows how a more accurate estimate for CAS results in a significantly improved along track predictions

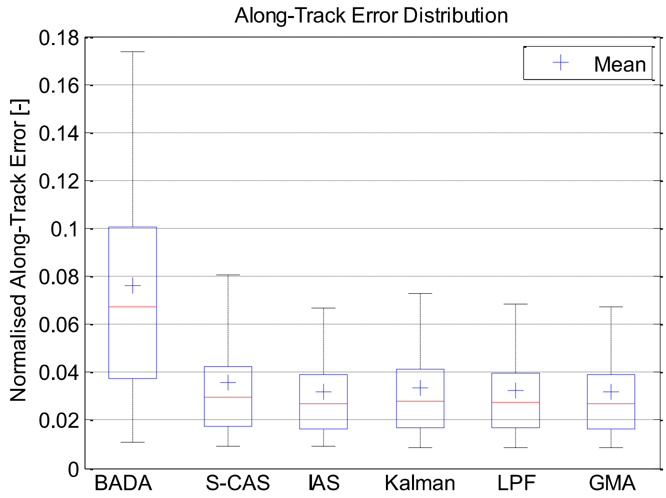

Figure 9 Along Track Errors

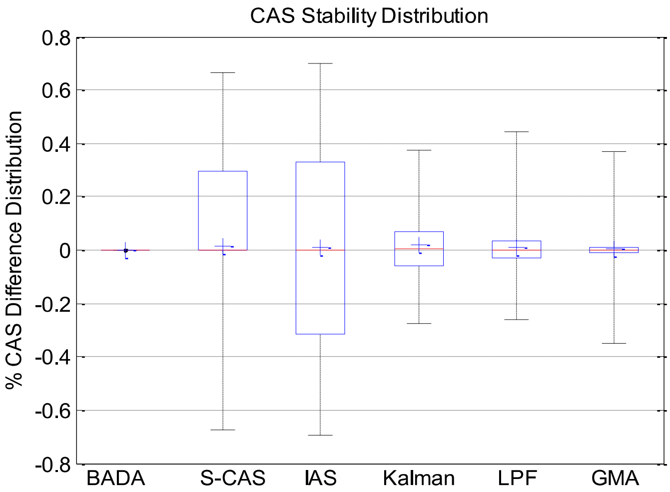

Figure 10 CAS stability results

generated by the TP. A value for CAS which fluctuates is likely to result in predictions where the along track position over time may vary accordingly from one prediction to the next. This can have a significant impact on relative geometries for given times when multiple aircraft trajectories are compared. It is anticipated that a value for CAS which does not fluctuate will generate

The CAS stability is calculated according to (4). The current CAS value is compared to the previous one. The relative increase or decrease in CAS is the metric. One sample was used per prediction point.

$$\varepsilon n = 100 \times \frac{CAS_n - CAS_{n-1}}{CAS_n} \quad (4)$$

The results for this metric are shown in Figure 10. The BADA baseline has a value of 0 which is to be expected as a single value is chosen for the whole climb. The S-CAS algorithm generated an interesting shape as the median coincides with the 0% line. This means at least a quarter of the predictions had a 0% CAS stability value. This is not surprising as the algorithm reverted back to BADA CAS when the Mode S IAS is not stable. The S-CAS approach also shows the largest spread. This wide containment interval is easily explained by the switching from Mode S CAS to BADA CAS and back. These switches are expected to generate large relative errors.

The raw IAS shows as expected the largest variation in stability. The containment is similar to the S-CAS method. The Kalman filter model has a decidedly narrower interquartile range. The LPF and GMA approach are even narrower. The containment between Kalman, LPF and GMA is similar.

D. Vertical and Along Track Bias

The bias calculations are simple metrics to assess general trends in the TP behaviour. The metric consists of the fraction of prediction points that are either above or below the radar altitude profile. In a similar manner the prediction points that are early or late are counted as well and then the taken as a fraction of the total count.

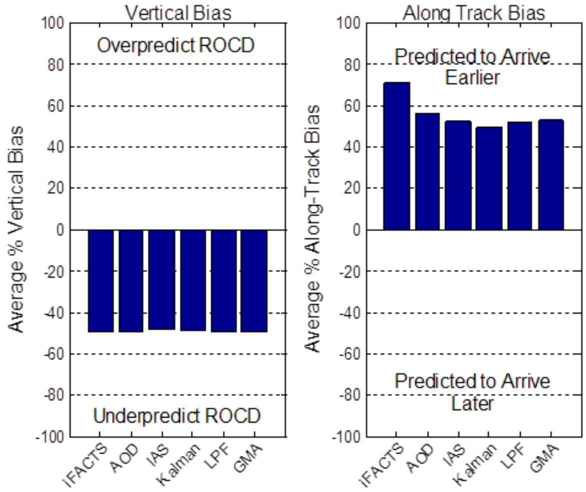

Figure 11 Vertical and Along Track Prediction bias

Figure 11 shows that there is a clear negative vertical bias which equates to all the algorithms predicting a profile which is mainly below the actual flight path. The along track metric shows a positive bias. This positive bias indicates that the majority of predictions are ahead of the actual aircraft behaviour.

IV. DISCUSSION

The results showed that all the methods of incorporating Mode S IAS in the TP calculations had an effect on accuracy and stability against the baseline BADA approach. The normalised vertical error did not change significantly, but all approaches which included Mode S IAS showed a significant improvement of the along track accuracy. The results are also more contained.

Since including the Mode S IAS to generate an estimate for the CAS changed the value from prediction to prediction the stability of the CAS value deteriorated as expected. The raw IAS showed the worst results and largest spread. The second worst performing was the S-CAS approach despite a large subset of the predictions showing a good, 0% CAS variability. The containment between the 5th and 95th percentile of the latter approaches was comparable. The Kalman, LPF and GMA approach showed significantly less variation and narrower containment intervals which indicated a more stable CAS value.

The nature of the downlinked Mode S IAS shows the variability of the signal. This means a trade-off needs to be sought between CAS stability and prediction accuracy.

All the predictions, baseline and new methods, shared the same bias of under predicting the vertical profile and over predicting the along track progress against radar observations. In the investigated sample the actual climb profiles flown by the aircraft tended to be steeper than the predictions.

This section discusses the relevance of these metrics and results on the controllers tools used in the NATS operation and the expected impact of some of these improvements on the controller tools

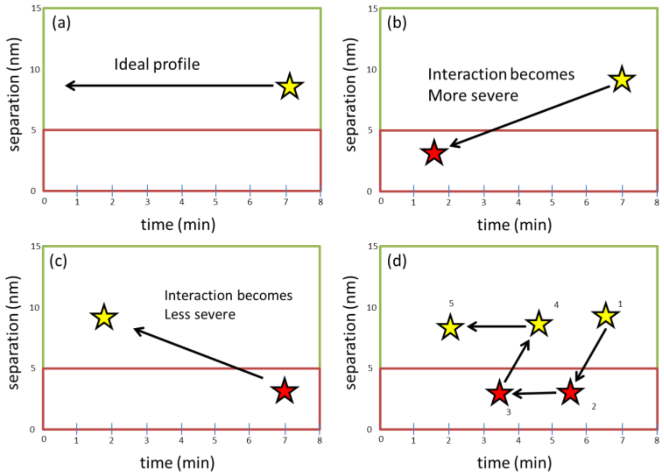

Figure 12 Separation Monitor examples: (a) shows the ideal behaviour of an interaction; (b) and (c) show the effect of accuracy on the prediction on the interaction - The interaction gets gradually better or worse; (d) shows the behaviour of an unstable interaction

General consensus for ATC human factors is to manage the ATCO workload to ensure it is kept at the right level. Figure 12 shows a set of distilled situations on the separation monitor. Sub plots (a), (b) and (d) show an interaction indicating that in nine minutes time, two aircraft will have their closest approach point (CAP) where they are separated by 7nm. In the ideal situation (a), as time moves on, the interaction will move to the left and eventually, when the two aircraft diverge again, the interaction disappears. If this situation is assured, the ATCO merely has to monitor this interaction until it disappears.

Figure 12 (b) & (c) show the effect of along-track imperfect accuracy on the interaction on the separation monitor. Reduced accuracy in a prediction can cause severe interactions to become less severe, but also the other way around, less severe actions to become more severe. Situation (c) will lead to an inconvenience for the ATCO where the cause of the interaction needs to be established and in the worst case an unnecessary clearance is issued resulting in a suboptimal use of airspace. The situation shown in (b) can have safety implications causing the ATCO to have to act reactively to avoid a loss of separation.

The underlying effect of this behaviour is the need for the ATCO to adapt to using the tools. The behaviour caused by the uncertainty means that the ATCO will probably spend more time monitoring these interactions causing more workload and reducing the number of aircraft that the ATCO can handle at any given time.

Figure 12 (d) shows the effect of unstable trajectory predictions on the behaviour of an interaction on the separation monitor. The interaction moves from reasonably benign to a sever interaction and then reverts back to a benign interaction. Given potential large discontinuities in the value for CAS (i.e. when the algorithm reverts back to BADA CAS if no stable value can be extracted from Mode S IAS) this behaviour could occur instantaneously. In reality an ATCO is very likely to issue remedial action the moment the interaction becomes more severe despite this not being necessary. Again this leads to extra workload, suboptimal use of airspace, and reduced trust in the available tools.

The bias towards under prediction in the climb has an effect on airspace use and controller workload. When a prediction is used to judge how far an aeroplane should be allowed to climb whilst maintaining separation the ATCO will typically remain on the cautious side and re-assess the situation when the climb is underway. Typically an aeroplane will have a continuous climb, but to achieve this will need continuous active monitoring and multiple clearances to be issued which again increases the ATCO's workload.

The simple metrics do not constitute full fitness for purpose metrics. Optimising one or more metrics could cause issues elsewhere in the system. The results show that each method requires compromises. A decision on which method is chosen requires understanding what's important not just in terms of performance but also in a safety context.

Given that the solutions which provide a good balance between stability and accuracy are the LPF, Kalman and GMA approaches. Of these three approaches the LPF and GMA require more elaborate state models and mode switches. A Kalman filter on the other hand is a well understood, mathematical approach. The characteristics of the whole history of a state are maintained in one variable which makes the updates between iterations more straightforward. It is anticipated that these characteristics make for an easier validation.

The Kalman filter can also easily be expanded to cover multiple states. Including more available information can further improve accuracy, stability and bias.

V. Conclusions and Further Work

This study investigated the effect of five methods for including Mode S IAS in the trajectory prediction calculation for aircraft climbs. These five methods were tested on a limited data set and compared against the BADA baseline. Analysis of 715 flights showed that including Mode S IAS has no significant effect on the predicted accuracy of the vertical profile. The along track prediction does become significantly more accurate. Furthermore it was shown that including the Mode S IAS makes the CAS profile significantly less stable in all methods.

The controller tools need a combination of both accuracy of trajectory prediction. Of the five approaches the Kalman filter showed the most promise to provide a balance between accuracy and stability. Furthermore the Kalman filter is also simple to implement, straightforward to validate and provides the possibility to expand.

This has been a limited study which shows some promise in the field of improving TP metrics therefore it is recommended to expand on this research in the following ways:

- Expand the analysis to cover various seasons and more aircraft types and compare the results with the findings of this study. If the results are consistent,

implement the Kalman filter into the tools and validate with ATCOs
- Investigate the use of the Mode S ROCD to improve the vertical accuracy of the TP during climb in a similar way to how Mode S IAS is used
- Perform regression analysis using 'Big Data' concepts and investigate incorporation of this information in the Kalman filter and other parts of the TP algorithms.

ACKNOWLEDGMENT

Many thanks to Anthony, Ben, David, and Richard for reviewing the paper and providing useful feedback.

REFERENCES

[1] User Manual for the Base of Aircraft Data. Version 3.8. EEC Technical/Scientific Report No. 2010-003

[2] Sosovicka, R., Vesley, P., Svoboda, J. 2015. Estimation of aircraft performance parameters from ADS-C EPP data. Integrated Communication, Navigation, and Surveillance Conference (ICNS).

[3] Haugg, E., Poppe, M., Herr, S., Putz., Svoboda, J., Sosovicka, R. 2015 The usability of ADS-C EPP data for air traffic control applications. Digital Avionics Systems Conference (DASC), 2015 IEEE/AIAA 34th

[4] AIRBUS Consortium. 2016. Providing Effective Ground and Air Data Sharing Via EPP (PEGASE). SESAR Very Large Scale Demonstration Report. SESAR LSD.01.04.

[5] The European ATM Masterplan. 2015. *https://www.atmmasterplan.eu*

[6] J. Lopez-Leones, M.A. Vilaplana, E. Gallo, F.A. Navarro, and C. Querejeta. 2007 The aircraft intent description language: A key enabler for airground synchronization in trajectory-based operations. In Proceedings of the 26th IEEE/AIAA Digital Avionics Systems Conference. DASC, 2007.

[7] Alligier, R., Gianazza, D., Durand, N. 2015. Machine learning and mass estimation methods for ground-based aircraft climb prediction. Intelligent Transportation Systems, IEEE Transactions.

[8] Alligier, R., Gianazza, D., Durand, N. 2015. Machine Learning Applied to Airspeed Prediction During Climb. USA/Europe Air Traffic Management R&D Seminar, Lisbon, Portugal.

[9] Stone, E., Pearce, G. 2016 A network of mode-s receivers for routine acquisition of aircraft-derived meteorological data. Journal of Atmospheric and Oceanic Technology, 33(4): 757-768.

[10] Mirza, A., Ballard, S.P., Dance, S.L., Maisey, P., Rooney, G.G., Stone, E.K. 2016. Comparison of aircraft derived observations with in situ research aircraft measurements. Quarterly Journal of the Royal Meteorological Society.

[11] Richard A Coppenbarger, "Climb Trajectory Prediction Enhancement Using Airline Flight Planning Information," NASA, Moffett Field, CA, AIAA Journal AIAA-99-4147, 1999.

[12] FAA/Eurocontrol Cooperative R&D, "Action Plan 16 Common Trajectory Prediction Capability, Common Trajectory Prediction-Related Terminology," Washington DC., 2004.

[13] B. et. al. Musialek, "Literature Survey of Trajectory Predictor Technology," Department of Transportation, Federal Aviation Administration, Springfield, Virgina, DOT/FAA/TC-TN11/1, 2010.

[14] Australian Department of Defence, Defence Science and Technology Organisation Aeronautical Research Laboratory, "Aircraft Trajectory Generation A Literature Review," Melbourne, Victoria, Literature Review Aircraft Systems Technical Memorandum 121, 1989.

[15] R. A. Coppenbarger and G. Kanning, "Real-Time Data Link of Aircraft Parameters to the Center-TRACON Automation System (CTAS)," Santa Fe, NM., 2001.

[16] D. Thipphavong, "Analysis of Climb Trajectory Modeling for Separation Assurance Automation," in AIAA Guidance, Navigation and Control Conference and Exhibit, 2008.

[17] Civil Aviation Authority. (2015, April) CAP 493: Manual of Air Traffic Services Part 1. Document.

[18] Yong Ching Lim, Hon Keung Kwan, and Wan-Chi Siu, Trends in Digital Signal Processing: A Festschrift in Honour of A.G. Constantinides, 1st ed. Boca Raton, United States of America, Florida: Pan Stanford, 2015.

[19] Richard G Lyons, Understanding Digital Signal Processing, 3rd ed.: Prentice Hall, 2011.

[20] https://ccrma.stanford.edu/~jos/filters/filters.html. (2015, April) Centre for Computer Research in Music and Acoustics (CCRMA): Introduction to Digital Filters. [Online]. https://ccrma.stanford.edu/~jos/filters/filters.html

[21] Ramsey Faragher. (2012, August) University of Cambridge, Faculty of Computer Science & Technolgoy: Understanding the Basis of the Kalman Filter Via a Simple and Intuitive Derivation.

[22] B. D. O. Anderson and J. B. Moore, Optimal Filtering. New York: Dover, 2005.

AUTHOR BIOGRAPHIES

Bram Vandermeersch graduated from Delft University of Technology in 2004 with an MSc in Aerospace Engineering. After ten years in the defence simulation and training industry he took up a position with NATS in 2015. His main focus there is trajectory modelling, performance analysis and data science

Jonathan Marmont graduated from the University of Glasgow in 2016 with a MEng in Aeronautical Engineering having completed his final year project at the NATS R&D department. Since graduating he has returned to NATS to commence training as an Air Traffic Controller.